

Influence of Random Telegraph Noise on Quantum Bit Gate Operation

Jackson Likens¹, Sanjay Prabhakar¹, Ratan Lal² and Roderick Melnik²

¹*Department of Natural Science, D L Hubbard Center for Innovation, Loess Hill Research Center, Northwest Missouri State University, 800 University Drive, Maryville, MO 64468*

²*Department of Computer Science, Northwest Missouri State University, 800 University Drive, Maryville, MO 64468*

³*MS2Discovery Interdisciplinary Research Institute, M3AI Lab,*

Wilfrid Laurier University, 75 University Avenue, Waterloo, ON N3L 3V6, Canada

(Dated: Nov 3, 2022)

We consider the problem of analyzing spin-flip qubit gate operation in presence of Random Telegraph Noise (RTN). Our broad approach is the following. We calculate the spin-flip probability of qubit driven by composite pulses, (Constant pulse (C-pulse), Quantum Well pulse (QW-pulse) and Barrier Potential pulse (BP-pulse)) in the presence of RTN using Feynman disentangling method. When composite pulses and RTN act in x-direction and z-direction respectively, we calculate the optimal time to achieve 100% spin-flip probability of qubit. We report the shortcut of spin-flip qubit, which can be achieved by using C-pulse, followed by BP-pulse and QW-pulse. When jumps time in RTN are very fast, tuning of perfect fidelity or spin-flip probability extends to large RTN correlation time. On the other hand, when the jumps in RTN are very slow, the BP-pulse can be used to recover the lost fidelities. Nevertheless, the fidelities of qubit gate operation are larger than 90%, regardless of RTN jumps environments which may be beneficial in quantum error correction. For more general case, we have tested several pulse sequences for achieving high fidelity quantum gates, where we have used the pulses acting in different directions. From the calculations, we find high fidelity of qubit gate operation in presence of RTN is achieved when QW-pulse, BP-pulse and C-pulse act in x-direction, y-direction and z-direction, respectively.

I. INTRODUCTION

Qubits can be manipulated in a desired fashion by excellent architect design in several physical devices, such as, quantum dots, cavity quantum electrodynamics, superconducting devices, Majorana fermions [1–17]. Manipulation of qubits in these devices seems promising in that one can make quantum logic gates and memory devices for various quantum information processing applications. Such devices require sufficiently short gate operation time combined with long coherent time [18–21].

When a qubit is operated on by a classical bit, then its decay time is given by a relaxation time which is also supposed to be longer than the minimum time required to execute one quantum gate operation. International Technology Roadmap for Semiconductors (ITRS) suggests that the node length and gate oxide thickness in CMOS technology for qubit gate operation is approaching approximately to one nanometer. Hence, a leakage current from source to drain through channel as well as gate to the channel through gate oxide layer is unavoidable. As a result recent experimental observations in the oscillations of drain current at both low and room temperatures confirms the origin of Random Telegraph Noise (RTN) that may reduce the performance of qubit gate operations [22–26]

In most cases, compared to coherent time, the dephasing time of qubits in presence of noise is reduced by several orders of magnitude due to coupling of qubits to the environment. The reduction of dephasing time depends on the specific dynamical coupling sequence from where the principle of quantum mechanics is inevitably lost. Therefore, one might need to decouple the qubits from

the environment and may consider more robust topological method to preserve a quantum state, enabling robust quantum memory [6, 27] Hence, to make quantum computers, one needs to find an efficient and experimentally feasible algorithm that overcome the issues of undesired interactions of qubits with RTN or the environment because these interactions destroy the quantum coherence that lead to generate errors and loss of fidelity. In quantum computing language, this phenomenon is called decoherence. For example, experimental observations reported that in GaAs quantum dots, decoherence time, $T_2^* \approx 10ns$ and coherent time, $T_1 \approx 0.1ms$, whereas for Si, $T_2^* \approx 100ns$ and $T_1 \approx 0.1ms$ [28–40]. There are several possible ways to overcome the issues of decoherence, as for example, fidelity recovery by applying error-correcting codes, decoherence free subspace coding, noiseless subsystem coding, dynamical decoupling from hot bath, numerical design of pulse sequences, that is more robust to experimental inhomogeneities, and optimal control pulse based on Markovian master equation descriptions [41–55].

In this paper, we design several control pulses acting on a single bit-flip computational basis states in presence of Random Telegraph Noise (RTN). Note that the choice of modeling parameters for RTN is same as that of experimentally observed RTN in Ref [22]. For example, choosing small noise correlation time in RTN provides very fast jumps, less than one tenth of picosecond of amplitude in RTN, whereas large noise correlation time provides slow jumps, larger than about 2 picosecond in RTN. Hence, checking performance of qubit under RTN in this paper resembles the realistic form of RTN that recently discussed in experimental studies in Ref. [22]. The present work identifies different regimes of operating pa-

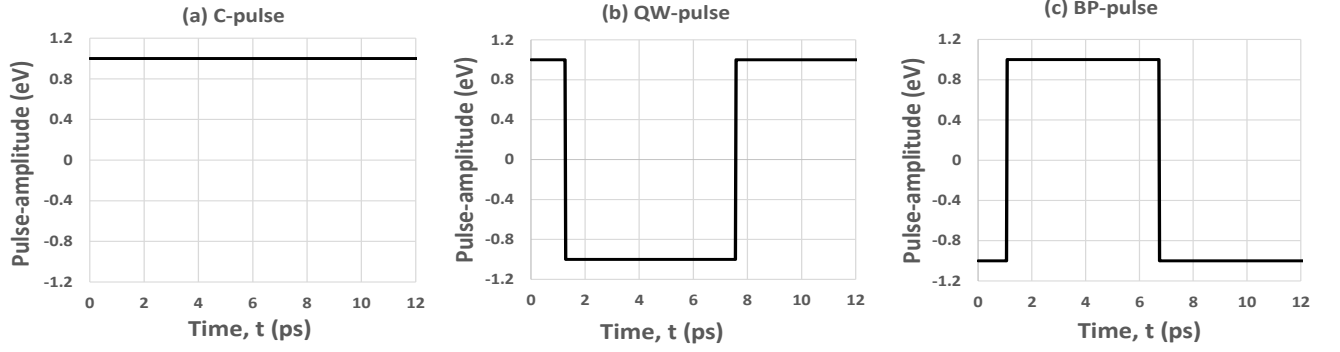


FIG. 1. The designed pulses for (a) C-pulse, (b) QW-pulse, and (c) BP-pulse that operate on qubit to achieve high fidelity quantum gates under random telegraph noise. The functional form of these pulses are shown in Eqs. (2) and (3). We chose $t_0 = 8\text{ps}$ for C-pulse, $t_0 = 1.8\text{ps}$ and $r_0 = -0.6$ for BP-pulse and $t_0 = 2.0\text{ps}$ and $r_0 = 2.56$ for QW-pulse.

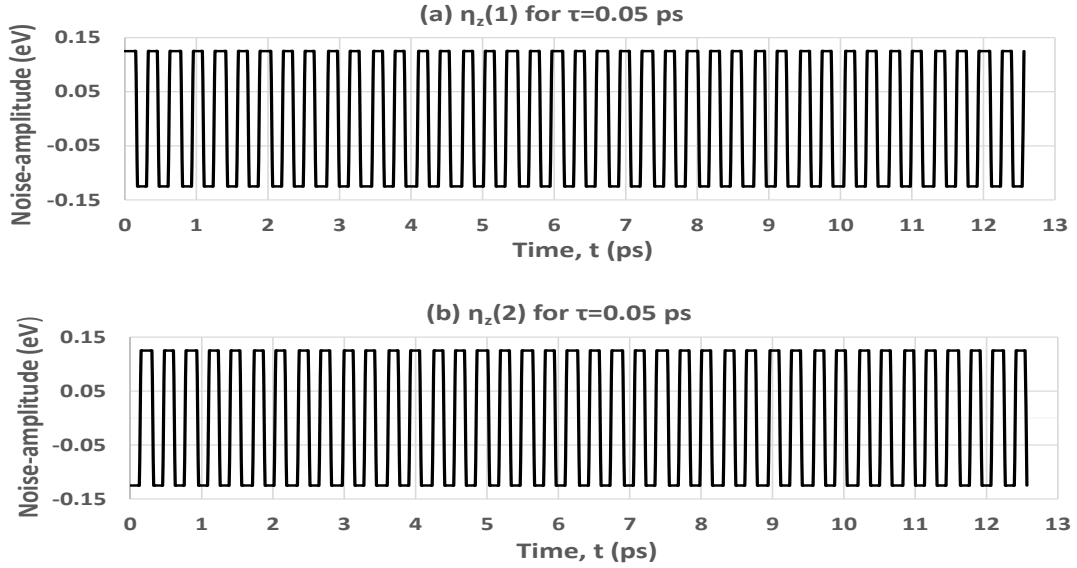


FIG. 2. Simulations of random telegraph noise (RTN) as a function of time are obtained from Eq. (4). Here we chose the correlation time $\tau_C = 0.05\text{ps}$ and $\Delta = 0.125\text{eV}$. Note that the density of RTN jumps between $\pm\Delta$ is random that is shown in Fig.2(a) and (b). Here only two RTN functions are shown for demonstration purpose but in a realistic simulations of finding high fidelity of spin-flip quantum gates, 300 RTN trajectories have been chosen.)

rameters in the designed control pulses that eliminate the series of phase and dynamical errors and increase the recovery of high fidelities of spin-flip qubit gate operation. The designed composite pulses, that we named, are Constant pulse (C-pulse), Quantum Well pulse (QW-pulse) and Barrier Potential pulse (BP-pulse), eventually acting on a qubit in presence of Random Telegraph Noise (RTN). The amplitude of C-pulse is constant with time, whereas three composite pulse sequences of different time width form QW-pulse and BP-pulse. The calculations of spin-flip qubit gate operation under RTN at various noise correlation times as well as various energy amplitudes of noise strength provide an indication of most efficient way to perform algorithm for achieving high fi-

delity quantum gates for quantum circuits and quantum error correction. In this paper, we report that when the qubits are driven by pulses in the x-direction and the RTN act in the z-direction then the C-pulse induce less systematic errors over QW-pulse and BP-pulse. For a more general case, we have tested all the possible combinations of the pulses acting in arbitrary x, y and z directions in presence of RTN and show that maximum fidelity of qubit gate operation can be achieved if C-pulse acts in x-direction, BP-pulse acts in y-direction and QW-pulse acts in z-direction. This useful information may be utilized to identify experimentally feasible pulses in presence of RTN for the design of next generation quantum circuits.

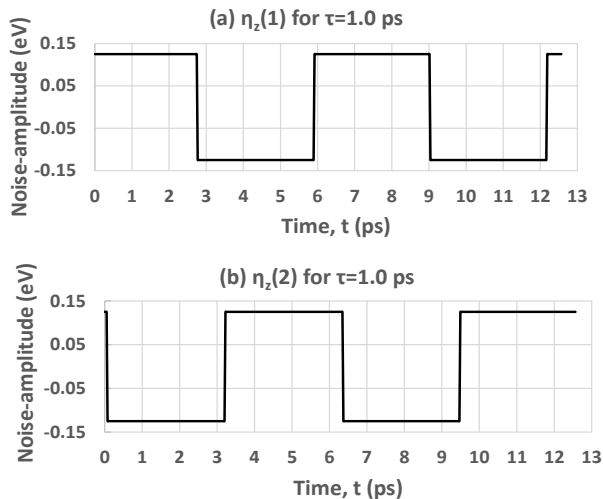


FIG. 3. Same as to Fig. 2 but $\tau_c = 1.0$ ps. Notice that the jumps in RTN is significantly decreased as correlation time, τ_c increases from 0.05ps in Fig. 2 to 1.0ps in Fig. 3. For large $\tau_c \approx 5.0$ ps, there are almost no jumps in RTN function and thus RTN can be treated as a white noise for large RTN correlation time.

The paper is organized as follows. In section II, we provide a theoretical description of finding exact unitary operator using Feynman Disentangling operator scheme of the model Hamiltonian of a qubit driven by several control pulses in presence of RTN. In section III, we analyze two main results: (i) fidelity of qubits driven by a pulse in the x-direction and RTN in z-direction. and (ii) the fidelity of qubits driven by individual pulses that act in the x,y and z-direction and the RTN still in the z-direction. Finally we conclude the results in Section IV.

II. MODEL HAMILTONIAN

The Hamiltonian of a single qubit is written as [56]

$$H(t) = \sum_{i \in \{x,y,z\}} \frac{1}{2} [a_i(t) + \eta_i(t)] \cdot \sigma_i, \quad (1)$$

where $a_i(t)$ is the energy amplitude of the external control pulse, $\eta_i(t)$ is the energy amplitude of the Random Telegraph Noise and σ_i is the Pauli spin matrices. Our goal is to design several composite pulses that provide high probability of spin-flip qubit in presence of RTN. Hence, we model the mathematical function of pulses as:

$$a_C(t) = \frac{\cos(t/t_0)}{|\cos(t/t_0)|}, \quad (2)$$

where $t_0 = 8$ ps for C-pulse. For BP and QW composite pulses, we model the function as:

$$a_{BP/QW}(t) = \frac{\sin(t/t_0 + r_0)}{|\sin(t/t_0 + r_0)|}, \quad (3)$$

where $t_0 = 1.8$ ps and $r_0 = -0.6$ for BP-pulse and $t_0 = 2.0$ ps and $r_0 = 2.56$ for QW-pulse. The designed C-pulse, BP-pulse and QW-pulse obtained from Eqs. (2) and (3) are shown in Fig. 1. Notice that amplitude of C-pulse is constant whereas combination of three composite pulses that form QW-pulse is shown in Fig. 1(b) and the combination of three composite pulses that form BP-pulse sequence is shown in Fig. 1(c). In the Hamiltonian (1), the RTN only acts in the z-direction because random RTN jumps originated mostly due to leakage current from gate oxide to the channel as spins are transported from source to drain, as demonstrated experimentally in [22]. The energy amplitude of the RTN changes randomly between $-\Delta$ and Δ , where Δ is the maximum energy amplitude. Hence, we model the RTN trajectory as:

$$\eta_z(t) = \Delta \frac{\sin(t/\tau - r_d)}{|\sin(t/\tau - r_d)|}, \quad (4)$$

where τ is RTN correlation time and $r_d = \log(p_i)$, where $p_i \in (0, 1)$ is the random numbers that determine the probability of random jumps of RTN trajectories. Two RTN functions are shown in Fig. 2 and 3. For the realistic simulations of spin-flip qubit, we have chosen 300 randomly generated RTN functions. As can be seen in Fig. 2, there are large density of RTN jumps in the vicinity of zero correlation times, τ_c . On the other hand, as τ_c increases, the density of RTN jumps decreases that can be seen in Fig. 3. Note that modeling parameters of RTN trajectories shown in Figs. 2 and 3 are in close vicinity of experimental trajectories of RTN reported in [22]. To find the system dynamics, average over different RTN sample trajectories is chosen to find the density matrix:

$$\rho(t) = \lim_{N \rightarrow \infty} \frac{1}{N} \sum_{k=1}^N U_k(t) \rho_0 U_k^\dagger(t), \quad (5)$$

where ρ_0 is the initial state of the system and $\{U_k\}$ is the unitary time evolution of the qubit under the influence of control pulses (see Fig. 1) and RTN (see Figs. 2 and 3). We write the unitary time evolution operator as

$$U_k(t) = T e^{-i/\hbar \int_0^t dt H(t)}, \quad (6)$$

where T is the time ordering parameter. We apply Feynman disentangling operators scheme and find the evolution operator as follows. The Hamiltonian, $H(t)$ in (1) or (6) can be written as

$$H(t) = H_+ s_+ + H_- s_- + H_z s_z, \quad (7)$$

where,

$$H_+ = \frac{1}{2} (a_x(t) - i a_y(t)) \quad (8)$$

$$H_- = \frac{1}{2} (a_x(t) + i a_y(t)) \quad (9)$$

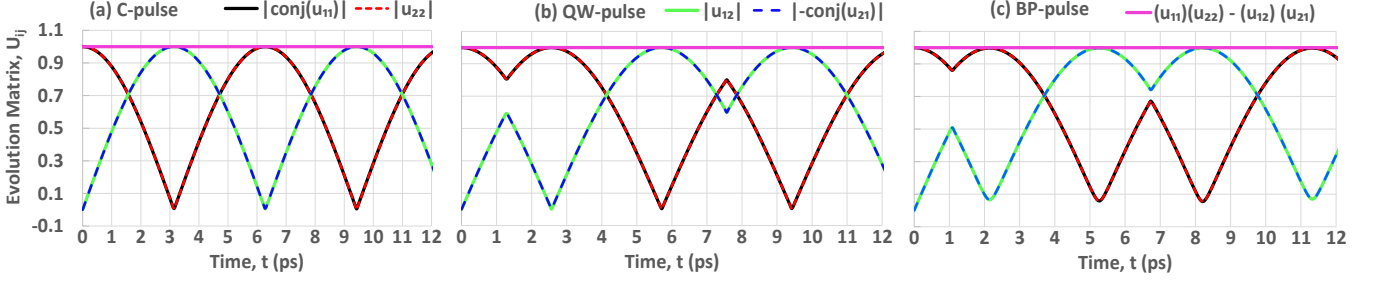


FIG. 4. Components of the evolution operator (see Eq. (33)) with respect to time for C-pulse in (a), QW-pulse in (b) and BP-pulse in (c). As can be seen in Figs.(a), (b) and (c), we find that $|u_{11}| = |u_{22}|$ and $|u_{12}| = |-u_{21}^*|$ as well as $(u_{11})(u_{22}) - (u_{12})(u_{21}) = 1$. Hence, we confirmed that the components of the unitary time evolution operator obtained from Feynman disentangling operator techniques are in good agreement to the theoretical descriptions of the evolution matrix in quantum mechanics.

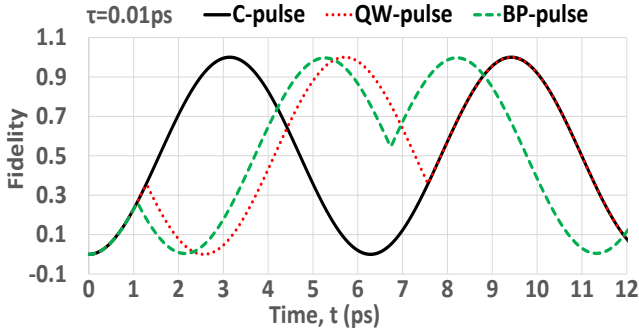


FIG. 5. (color online) Fidelity of spin-flip qubit, obtained from Eq. (34), as a function of RTN correlation time for C-pulse, QW-pulse and BP-pulse. Here, we chose $\Delta = 0.125eV$. As can be seen, tuning of perfect fidelity extends to large RTN correlation time for C-pulse due to short optimal gate operation time ($t = 3.14$ ps for C-pulse, $t = 9.42$ ps for QW-pulse and $t = 8.20$ ps for BP-pulse, see Fig. 5). At large RTN correlation time, where there is no jumps in RTN, BP-pulse can be used to recover the lost fidelities over other two pulses, (e.g. fidelity of BP-pulse is larger than C-pulse and QW-pulse at large RTN correlation time).

$$H_z = a_z(t) + \eta_z(t), \quad (10)$$

and $s_{\pm} = (\sigma_x \pm i\sigma_y)/2$ and $s_z = \sigma_z/2$. In the disentangled form, the unitary time evolution operator (6) can be written as

$$U_k(t) = \exp(\alpha(t)s_+) \exp(\beta(t)s_z) \exp(\gamma(t)s_-), \quad (11)$$

where $\alpha(t)$, $\beta(t)$ and $\gamma(t)$ are unknown that can be found by using Feynman disentangling operator calculus method [6, 8, 57, 58]. We write $H(t)$ of (7) as

$$H(t) = \xi s'_+ + (H_+ - \xi)s'_+ + H_z s'_z + H_- s'_-, \quad (12)$$

where

$$\alpha(t) = -\frac{i}{\hbar} \int_0^t \xi(t) dt, \quad (13)$$

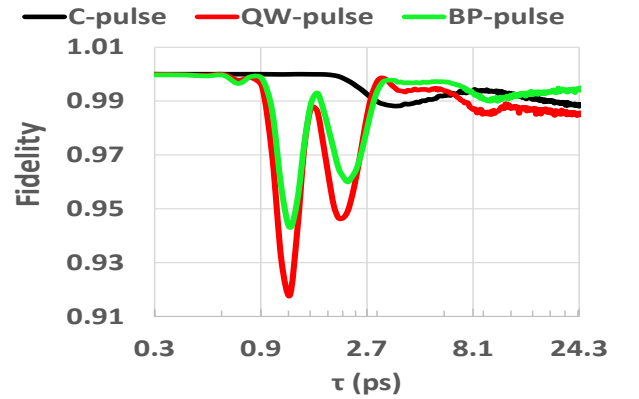


FIG. 6. (color online) Fidelity of spin-flip qubit as a function of RTN correlation time, τ for C-pulse, QW-pulse and BP-pulse. We chose $\Delta = 0.125 eV$. As can be seen, C-pulse extends tuning of perfect fidelity to large RTN correlation time because it possesses very short optimal time, $t = 3.14ps$ for spin-flip qubit gate operation. At large correlation time ($\tau \approx 20ps$), recovery of fidelity for BP-pulse is higher than all the other pulses.

$$s'_\mu(t) = \exp(-\alpha s_+) s_\mu \exp(\alpha s_+). \quad (14)$$

Differentiating Eq. (14) with respect to α , we can write

$$\frac{ds'_\mu(t)}{d\alpha} = \exp(-\alpha s_+) [s_\mu, s_+] s_\mu \exp(\alpha s_+), \quad (15)$$

and utilizing initial condition, $s'_\mu(0) = s_\mu$, we find $s'_+ = s_+$, $s'_0 = s_0 + s_+ \alpha$, $s'_- = s_- - s_+ \alpha^2 - 2s_0 \alpha$. Substituting Eq. (12) in Eq. (6), we can write the unitary time evolution operator as

$$U_k(t) = e^{\alpha(t)s_+} T e^{-\frac{i}{\hbar} h(\alpha) dt}, \quad (16)$$

where

$$h(\alpha) = (H_+ - \xi + H_z \alpha - H_- \alpha^2) s_+ + H_z s_z + H_- s_- - 2H_- s_- \alpha. \quad (17)$$

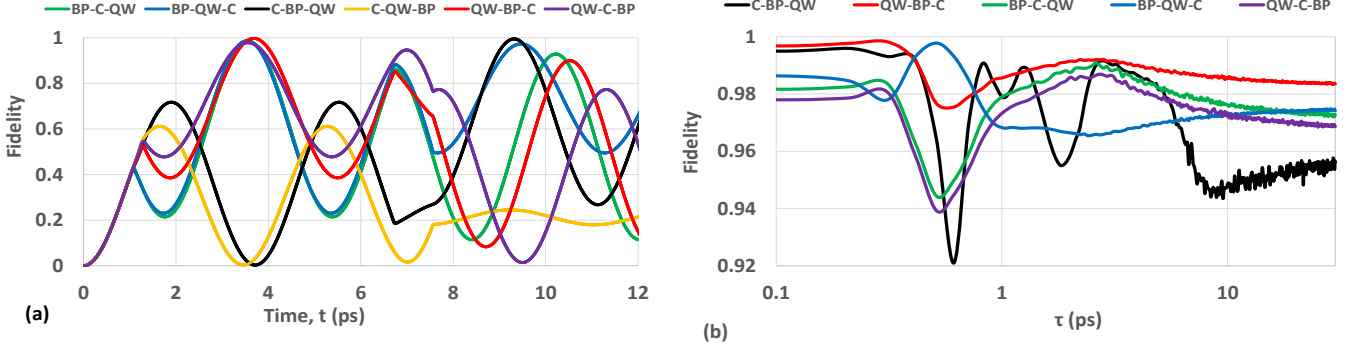


FIG. 7. (a) Fidelity of spin-flip qubit as a function of time for the pulse sequences shown in the systematic orders, e.g. for BP-C-QW pulse sequence, BP-pulse acts in x-direction, C-pulse acts in y-direction and QW-pulse acts in z-direction. As can be seen the optimal time pulse for BP-C-QW is 3.57ps, for BP-QW-C is 3.53ps, C-BP-QW is 9.46ps, QW-BP-C is 3.66ps and QW-C-BP is 3.57ps. For the C-QW-BP pulse, fidelity is very small and may not be useful for achieving high fidelity quantum gates. (b) Fidelity of spin-flip qubit as a function of RTN correlation time, τ for $\Delta = 0.125 eV$ for several pulse sequences is shown. As can be seen QW-BP-C pulse has better performance than all the other pulses for achieving high fidelity quantum gates with respect to RTN correlation time. Nevertheless the fidelities for all the pulses shown in Fig. 7(b) is larger than 92%. Such small error induced by RTN can be corrected for application in qubit gate operation.

Equating coefficient of s_+ to zero, we write

$$\frac{d\alpha}{dt} = -\frac{i}{\hbar} \left[\frac{1}{2} (a_x - ia_y) + (a_z + \eta_z) \alpha - \frac{1}{2} (a_x + ia_y) \alpha^2 \right]. \quad (18)$$

Hence, s_+ of (17) in (16) is completely disentangled and thus unitary time evolution operator ((16)) can be written in the disentangled form as

$$U_k(t) = e^{\alpha(t)s_+} T e^{-\frac{i}{\hbar} \int_0^t H'(s'_\mu, \alpha) dt}, \quad (19)$$

where,

$$H'(s'_\mu, \alpha) = \zeta s'_z + (H_z - 2H_- \alpha - \zeta) s'_z + H_- s'_-. \quad (20)$$

$$\beta(t) = -\frac{i}{\hbar} \int_0^t \zeta(t) dt, \quad (21)$$

$$s'_\mu(t) = \exp(-\alpha s_z) s_\mu \exp(\alpha s_z). \quad (22)$$

Differentiating Eq. (22) with respect to β , we can write

$$\frac{ds'_\mu(t)}{d\alpha} = \exp(-\alpha s_z) [s_\mu, s_z] s_\mu \exp(\alpha s_z), \quad (23)$$

and utilizing initial condition, $s'_\mu(0) = s_\mu$, we find $s'_z = s_z$, $s'_- = s_- \exp(\beta)$. Substituting Eq. (20) in Eq. (19), we can write the unitary time evolution operator as

$$U_k(t) = e^{\alpha(t)s_+} e^{\beta(t)s_z} T e^{-\frac{i}{\hbar} [(H_0 - 2H_- \alpha - H_- \zeta) s_z + H_- s_-] dt}. \quad (24)$$

Equating coefficient of s_z to zero, we write

$$\frac{d\beta}{dt} = -\frac{i}{\hbar} [a_z + \eta_z - (a_x + ia_y)]. \quad (25)$$

Hence, s_z of (24) is completely disentangled and thus unitary time evolution operator 24 can be written in the disentangled form as

$$U_k(t) = e^{\alpha(t)s_+} e^{\beta(t)s_z} T e^{-\frac{i}{\hbar} \int_0^t H''(s'_\mu, \alpha, \beta) dt}, \quad (26)$$

where,

$$H''(s'_\mu, \alpha, \beta) = \chi s'_- + (H_- e^\beta - \chi) s'_-. \quad (27)$$

$$\gamma(t) = -\frac{i}{\hbar} \int_0^t \chi(t) dt, \quad (28)$$

$$s'_\mu(t) = \exp(-\gamma s_-) s_\mu \exp(\alpha s_-). \quad (29)$$

Differentiating Eq. (29) with respect to γ , we can write

$$\frac{ds'_\mu(t)}{d\gamma} = \exp(-\gamma s_-) [s_\mu, s_-] s_\mu \exp(\alpha s_-), \quad (30)$$

and utilizing initial condition, $s'_\mu(0) = s_\mu$, we find $s'_- = s_-$. Substituting Eq. (27) in Eq. (24), we can write the unitary time evolution operator as

$$U_k(t) = e^{\alpha(t)s_+} e^{\beta(t)s_z} e^{\gamma(t)s_-} T e^{-\frac{i}{\hbar} [(H_- \exp(\beta) - \chi) s'_-] dt}. \quad (31)$$

Equating coefficient of s_z to zero, we write

$$\frac{d\gamma}{dt} = -\frac{i}{\hbar} \left[\frac{1}{2} (a_x + ia_y) \right]. \quad (32)$$

Hence, unitary time evolution operator (31) is completely disentangled. Finally, the exact unitary time evolution operator (31) can be written as

$$U_k(t) = \begin{pmatrix} \exp\left(\frac{\beta}{2}\right) + \alpha\gamma \exp\left\{-\frac{\beta}{2}\right\} & \alpha \exp\left(-\frac{\beta}{2}\right) \\ \gamma \exp\left(-\frac{\beta}{2}\right) & \exp\left(-\frac{\beta}{2}\right) \end{pmatrix}, \quad (33)$$

Since (33) is the exact time evolution operator in the disentangled form, we can construct the density matrix of (5) and find the fidelity of qubit as

$$\phi = \text{tr}\{\rho_f^\dagger \rho_T\}, \quad (34)$$

where $\rho_f = U_f \rho_0 U_f^\dagger$ is the final state of the system and ρ_T is the final desired state of the qubit, where the pulse sequence end. Here U_f is a quantum gate that is independent of the initial state preparation. In this paper, we chose U_f is a Pauli X-gate and prepare the initial state $|0\rangle = (0, 0, 0, 1)_{2 \times 2}$ and final state $|1\rangle = (1, 0, 0, 0)_{2 \times 2}$ and then find the spin-flip probability by using Eq. (34). In this paper, we use Feynman disentangling operator scheme [6, 8, 57, 58] to find the system dynamics of Eq. (6). We have chosen 300 RTN trajectories and $\hbar = a_{max} = 1$.

III. RESULTS AND DISCUSSIONS

In Fig. 4, we have plotted the components of the evolution operator (33) of C-pulse in (a), QW-pulse in (b) and BP-pulse in (c) for RTN correlation time, $\tau_C = 0.001\text{ps}$. The data in these plots show that $u_{22} = |\text{conj}(u_{11})|$ and $u_{12} = |-\text{conj}(u_{21})|$ for C-pulse, QW-pulse and BP-pulse as well as $|U_k(t, 0)| = 1$. Hence, we confirmed that the evolution matrix obtained from Feynman disentangling operator method is very accurate. In Fig. 5, we have plotted the fidelity of spin-flip qubit with respect to the evolution of time for C-pulse, QW-pulse and BP-pulse. As can be seen that the perfect fidelity can be achieved at $t = 3.14\text{ps}$ for C-pulse, $t = 9.42\text{ps}$ for QW-pulse and $t = 8.20\text{ps}$ for BP-pulse. We consider these times as the optimum time for achieving high fidelity of spin-flip qubit in presence of RTN. Notice that optimum time for spin-flip qubit is smallest for C-pulse (i.e., $t = 3.14\text{ps}$) but optimum time for BP-pulse is smaller (i.e., $t = 8.20\text{ps}$) than the QW-pulse (i.e., $t = 9.42\text{ps}$) because C-pulse has constant energy amplitude but width of the QW-pulse is larger than the width of BP-pulse (e.g., see Fig. 1). In other words, QW-pulse lasts longer than the BP-pulse during the spin-flip qubit gate operation.

We consider the C-pulse, QW-pulse and BP-pulse act in the x-direction and RTN in z-direction in the Hamiltonian (1) and plotted the fidelity of spin-flip qubit with respect to the RTN correlation time in Fig. 6. As can be seen in the regime of vanishing RTN correlation time (i.e., $\tau_c \rightarrow 0$), perfect fidelity can be observed for all the three pulses, e.g., C-pulse, QW-pulse and BP-pulse due to the fact that the single qubit does not have sufficiently large time to drift along the direction of densely populated random telegraph noise (see Fig. 2). Note that the RTN function is very dense in the vicinity of zero correlation time (see Fig.2) but has no jumps in the vicinity of infinite correlation time (e.g., density of noise jumps decreases as τ_c increases, see Fig.2 and Fig.3). In Fig. 6, we also observed oscillations in the intermediate regime

of RTN correlation time, (e.g., $\tau \approx 2.7\text{ps}$ for C-pulse and $\tau \approx 1.2\text{ps}$ for BP-pulse and QW-pulse) due to the fact that as the jumps in RTN slowed down then qubit stays in the RTN state that let the qubit to drift along the noise direction. For large RTN correlation time where RTN can be treated as a white noise, or there is no jumps in RTN, qubit recovers most of its lost fidelity. As can be seen, when RTN is treated as a white noise, BP-pulse has high fidelity than C-pulse and QW-pulse.

As shown in Fig. 7, for the pulses acting in all three directions and RTN in z-direction, we can achieved high fidelity of spin-flip qubit only when QW-pulse acts in x-direction, BP-pulse acts in y-direction and C-pulse acts in z-direction (red plot in Fig. 7(b)). Optimum time for such pulse sequences is $t = 3.66\text{ps}$ that can be achieved from fidelity of spin-flip qubit-vs-time in Fig. 7 (a). Note that we have tested all the other possible combinations of pulses as shown in Fig. 7(a) to achieve the optimal time for high fidelity of qubit. In Fig. 7(b), we have plotted the fidelity of spin-flip qubit with respect to the RTN correlation time. As can be seen, the fidelity of QW-BP-C pulse in presence of RTN has better performance than all the other sequences of the pulses but the fidelity of spin-flip qubit for all the other pulses are still above 90% and may still be used for quantum error correction and quantum information processing.

IV. CONCLUSION

We have shown a possible way to achieve high fidelity of spin-flip qubit gate operation using several control pulses (e.g., C-pulse, QW-pulse, and BP-pulse) in presence of random telegraph noises. In Fig. 6, in the limit of vanishing RTN correlation time, C-pulse can be used for the measurement of achieving high fidelity spin-flip qubit operation due to its small optimal gate operation time. In particular, for small values of RTN correlation time, C-pulse extends the tuning of perfect fidelity to large RTN correlation time. When the RTN correlation time is large (e.g., $\tau_C \rightarrow \text{inf}$), possibly white noise, BP-pulse can be used to achieve high fidelity of spin-flip qubit gate operation. In Fig. 7 when the pulses acting in all the three directions, we have tested several pulse sequences for achieving high fidelity quantum gates and report that QW-pulse acting in x-direction, BP-pulse acting in y-direction and C-pulse acting in z-direction can be used to provide high fidelity of qubit gate operation in presence of RTN. Regardless of RTN conditions, the fidelities of spin-flip qubit gate operations for these pulses are larger than 92%. Since the modeling parameters of RTN resembles with the experimentally observed RTN in Ref. [22], one can use QW-pulse, BP-pulse and C-pulse to transport the qubit for several different kinds of quantum gate operation that may have applications in solid state realization of quantum computing and quantum information processing.

V. ACKNOWLEDGEMENTS

The simulations are performed at BARTIK High-Performance Cluster (National Science Foundation Grant No. CNS-1624416, U.S.) in Northwest Missouri

State University. JL and SP acknowledge Northwest Missouri State University for providing financial support to present these results at American Physical Society March meeting in Chicago (2022). RM is acknowledging the support of NSERC Discovery and CRC Programs.

-
- [1] M.-S. Choi, C. Bruder, and D. Loss, Spin-dependent josephson current through double quantum dots and measurement of entangled electron states, *Physical review B* **62**, 13569 (2000).
- [2] G. Burkard, D. Loss, and D. P. DiVincenzo, Coupled quantum dots as quantum gates, *Physical Review B* **59**, 2070 (1999).
- [3] X. Hu and S. D. Sarma, Hilbert-space structure of a solid-state quantum computer: Two-electron states of a double-quantum-dot artificial molecule, *Physical Review A* **61**, 062301 (2000).
- [4] T. S. Koh, J. K. Gamble, M. Friesen, M. Eriksson, and S. Coppersmith, Pulse-gated quantum-dot hybrid qubit, *Physical review letters* **109**, 250503 (2012).
- [5] D. Xiao, M.-C. Chang, and Q. Niu, Berry phase effects on electronic properties, *Reviews of modern physics* **82**, 1959 (2010).
- [6] S. Prabhakar, J. Raynolds, A. Inomata, and R. Melnik, Manipulation of single electron spin in a gaas quantum dot through the application of geometric phases: The feynman disentangling technique, *Physical Review B* **82**, 195306 (2010).
- [7] S. Prabhakar, R. Melnik, and L. L. Bonilla, Gate control of berry phase in iii-v semiconductor quantum dots, *Physical Review B* **89**, 245310 (2014).
- [8] S. Prabhakar, R. Melnik, and A. Inomata, Geometric spin manipulation in semiconductor quantum dots, *Applied Physics Letters* **104**, 142411 (2014).
- [9] U. Vool, S. Shankar, S. Mundhada, N. Ofek, A. Narla, K. Sliwa, E. Zolys-Geller, Y. Liu, L. Frunzio, R. Schoelkopf, *et al.*, Continuous quantum nondemolition measurement of the transverse component of a qubit, *Physical Review Letters* **117**, 133601 (2016).
- [10] H.-K. Lau and M. B. Plenio, Universal continuous-variable quantum computation without cooling, *Physical Review A* **95**, 022303 (2017).
- [11] F. Yoshihara, T. Fuse, S. Ashhab, K. Kakuyanagi, S. Saito, and K. Semba, Superconducting qubit-oscillator circuit beyond the ultrastrong-coupling regime, *Nature Physics* **13**, 44 (2017).
- [12] D. J. Clarke, J. D. Sau, and S. D. Sarma, A practical phase gate for producing bell violations in majorana wires, *Physical Review X* **6**, 021005 (2016).
- [13] L. Grünhaupt, M. Spiecker, D. Gusenkova, N. Maleeva, S. T. Skacel, I. Takmakov, F. Valenti, P. Winkel, H. Rotzinger, W. Wernsdorfer, *et al.*, Granular aluminium as a superconducting material for high-impedance quantum circuits, *Nature materials* **18**, 816 (2019).
- [14] Y. Zhong, H.-S. Chang, K. Satzinger, M.-H. Chou, A. Bienfait, C. Conner, É. Dumur, J. Grebel, G. Peairs, R. Povey, *et al.*, Violating bell's inequality with remotely connected superconducting qubits, *Nature Physics* **15**, 741 (2019).
- [15] P. Kurpiers, M. Pechal, B. Royer, P. Magnard, T. Walter, J. Heinsoo, Y. Salathé, A. Akin, S. Storz, J.-C. Besse, *et al.*, Quantum communication with time-bin encoded microwave photons, *Physical Review Applied* **12**, 044067 (2019).
- [16] Y. Xu, W. Cai, Y. Ma, X. Mu, L. Hu, T. Chen, H. Wang, Y. Song, Z.-Y. Xue, Z.-q. Yin, *et al.*, Single-loop realization of arbitrary nonadiabatic holonomic single-qubit quantum gates in a superconducting circuit, *Physical review letters* **121**, 110501 (2018).
- [17] X. Li, Y. Ma, J. Han, T. Chen, Y. Xu, W. Cai, H. Wang, Y. Song, Z.-Y. Xue, Z.-q. Yin, *et al.*, Perfect quantum state transfer in a superconducting qubit chain with parametrically tunable couplings, *Physical Review Applied* **10**, 054009 (2018).
- [18] D. Loss and D. P. DiVincenzo, Quantum computation with quantum dots, *Physical Review A* **57**, 120 (1998).
- [19] V. N. Golovach, A. Khaetskii, and D. Loss, Phonon-induced decay of the electron spin in quantum dots, *Phys. Rev. Lett.* **93**, 016601 (2004).
- [20] S. Amasha, K. MacLean, I. P. Radu, D. Zumbühl, M. Kastner, M. Hanson, A. Gossard, Electrical control of spin relaxation in a quantum dot, *Physical review letters* **100**, 046803 (2008).
- [21] A. Balocchi, Q. Duong, P. Renucci, B. Liu, C. Fontaine, T. Amand, D. Lagarde, and X. Marie, Full electrical control of the electron spin relaxation in gaas quantum wells, *Physical review letters* **107**, 136604 (2011).
- [22] Z. Li, M. Sotto, F. Liu, M. K. Husain, H. Yoshimoto, Y. Sasago, D. Hisamoto, I. Tomita, Y. Tsuchiya, and S. Saito, Random telegraph noise from resonant tunnelling at low temperatures, *Scientific reports* **8**, 1 (2018).
- [23] F. Liu, K. Ibukuro, M. K. Husain, Z. Li, J. Hillier, I. Tomita, Y. Tsuchiya, H. Rutt, and S. Saito, Manipulation of random telegraph signals in a silicon nanowire transistor with a triple gate, *Nanotechnology* **29**, 475201 (2018).
- [24] S. Singh, E. T. Mannila, D. S. Golubev, J. T. Peltonen, and J. P. Pekola, Determining the parameters of a random telegraph signal by digital low pass filtering, *Applied Physics Letters* **112**, 243101 (2018).
- [25] X. Zhan, Y. Xi, Q. Wang, W. Zhang, Z. Ji, and J. Chen, Dual-point technique for multi-trap rtn signal extraction, *IEEE Access* **8**, 88141 (2020).
- [26] H. Yang, M. Robitaille, X. Chen, H. Elgabra, L. Wei, and N. Y. Kim, Random telegraph noise of a 28-nm cryogenic mosfet in the coulomb blockade regime, *IEEE Electron Device Letters* **43**, 5 (2021).
- [27] J. Jing, L.-A. Wu, M. Byrd, J. Q. You, T. Yu, and Z.-M. Wang, Nonperturbative leakage elimination operators and control of a three-level system, *Phys. Rev. Lett.* **114**, 190502 (2015).
- [28] H. Bluhm, S. Foletti, I. Neder, M. Rudner, D. Mahalu, V. Umansky, and A. Yacoby, Dephasing time of gaas

- electron-spin qubits coupled to a nuclear bath exceeding 200 [thinsp][mu] s, *Nature Physics* **7**, 109 (2011).
- [29] J. R. Petta, A. C. Johnson, J. M. Taylor, E. A. Laird, A. Yacoby, M. D. Lukin, C. M. Marcus, M. P. Hanson, and A. C. Gossard, Coherent manipulation of coupled electron spins in semiconductor quantum dots, *Science* **309**, 2180 (2005).
- [30] B. M. Maune, M. G. Borselli, B. Huang, T. D. Ladd, P. W. Deelman, K. S. Holabird, A. A. Kiselev, I. Alvarado-Rodriguez, R. S. Ross, A. E. Schmitz, *et al.*, Coherent singlet-triplet oscillations in a silicon-based double quantum dot, *Nature* **481**, 344 (2012).
- [31] J. J. Pla, K. Y. Tan, J. P. Dehollain, W. H. Lim, J. J. Morton, D. N. Jamieson, A. S. Dzurak, and A. Morello, A single-atom electron spin qubit in silicon, *Nature* **489**, 541 (2012).
- [32] F. K. Malinowski, F. Martins, T. B. Smith, S. D. Bartlett, A. C. Doherty, P. D. Nissen, S. Fallahi, G. C. Gardner, M. J. Manfra, C. M. Marcus, *et al.*, Spin of a multielectron quantum dot and its interaction with a neighboring electron, *Physical Review X* **8**, 011045 (2018).
- [33] M. Friesen, J. Ghosh, M. Eriksson, and S. Coppersmith, A decoherence-free subspace in a charge quadrupole qubit, *Nature communications* **8**, 15923 (2017).
- [34] F. Martins, F. K. Malinowski, P. D. Nissen, S. Fallahi, G. C. Gardner, M. J. Manfra, C. M. Marcus, and F. Kuemmeth, Negative spin exchange in a multielectron quantum dot, *Physical review letters* **119**, 227701 (2017).
- [35] Y. He, S. Gorman, D. Keith, L. Kranz, J. Keizer, and M. Simmons, A two-qubit gate between phosphorus donor electrons in silicon, *Nature* **571**, 371 (2019).
- [36] J. Geng, Y. Wu, X. Wang, K. Xu, F. Shi, Y. Xie, X. Rong, and J. Du, Experimental time-optimal universal control of spin qubits in solids, *Physical review letters* **117**, 170501 (2016).
- [37] B.-J. Liu, X.-K. Song, Z.-Y. Xue, X. Wang, and M.-H. Yung, Plug-and-play approach to nonadiabatic geometric quantum gates, *Physical Review Letters* **123**, 100501 (2019).
- [38] R. E. Throckmorton, E. Barnes, and S. D. Sarma, Environmental noise effects on entanglement fidelity of exchange-coupled semiconductor spin qubits, *Physical Review B* **95**, 085405 (2017).
- [39] X.-C. Yang, M.-H. Yung, and X. Wang, Neural-network-designed pulse sequences for robust control of singlet-triplet qubits, *Physical Review A* **97**, 042324 (2018).
- [40] C.-H. Huang and H.-S. Goan, Robust quantum gates for stochastic time-varying noise, *Physical Review A* **95**, 062325 (2017).
- [41] N. Ofek, A. Petrenko, R. Heeres, P. Reinhold, Z. Leghtas, B. Vlastakis, Y. Liu, L. Frunzio, S. Girvin, L. Jiang, *et al.*, Extending the lifetime of a quantum bit with error correction in superconducting circuits, *Nature* **536**, 441 (2016).
- [42] M. H. Michael, M. Silveri, R. Brierley, V. V. Albert, J. Salmilehto, L. Jiang, and S. M. Girvin, New class of quantum error-correcting codes for a bosonic mode, *Physical Review X* **6**, 031006 (2016).
- [43] B. J. Brown, D. Loss, J. K. Pachos, C. N. Self, and J. R. Wootton, Quantum memories at finite temperature, *Reviews of Modern Physics* **88**, 045005 (2016).
- [44] A. Reiserer, N. Kalb, M. S. Blok, K. J. van Bemmelen, T. H. Taminiau, R. Hanson, D. J. Twitchen, and M. Markham, Robust quantum-network memory using decoherence-protected subspaces of nuclear spins, *Physical Review X* **6**, 021040 (2016).
- [45] H.-K. Lau and M. B. Plenio, Universal quantum computing with arbitrary continuous-variable encoding, *Physical Review Letters* **117**, 100501 (2016).
- [46] B.-H. Liu, X.-M. Hu, J.-S. Chen, C. Zhang, Y.-F. Huang, C.-F. Li, G.-C. Guo, G. b. u. Karpat, F. F. Fanchini, J. Piilo, and S. Maniscalco, Time-invariant entanglement and sudden death of nonlocality, *Phys. Rev. A* **94**, 062107 (2016).
- [47] A. Castro, J. Werschnik, and E. K. Gross, Controlling the dynamics of many-electron systems from first principles: a combination of optimal control and time-dependent density-functional theory, *Physical review letters* **109**, 153603 (2012).
- [48] X. Wang, L. S. Bishop, J. Kestner, E. Barnes, K. Sun, and S. D. Sarma, Composite pulses for robust universal control of singlet-triplet qubits, *Nature communications* **3**, 997 (2012).
- [49] M. Jenei, E. Potanina, R. Zhao, K. Y. Tan, A. Rossi, T. Tanttu, K. W. Chan, V. Sevriuk, M. Möttönen, and A. Dzurak, Waiting time distributions in a two-level fluctuator coupled to a superconducting charge detector, *Phys. Rev. Research* **1**, 033163 (2019).
- [50] S. L. Rudge and D. S. Kosov, Fluctuating-time and full counting statistics for quantum transport in a system with internal telegraphic noise, *Phys. Rev. B* **100**, 235430 (2019).
- [51] F. Motzoi, E. Halperin, X. Wang, K. B. Whaley, and S. Schirmer, Backaction-driven, robust, steady-state long-distance qubit entanglement over lossy channels, *Phys. Rev. A* **94**, 032313 (2016).
- [52] C. Dickel, J. J. Westdorp, N. K. Langford, S. Peiter, R. Sagastizabal, A. Bruno, B. Criger, F. Motzoi, and L. DiCarlo, Chip-to-chip entanglement of transmon qubits using engineered measurement fields, *Phys. Rev. B* **97**, 064508 (2018).
- [53] P. Kurpiers, P. Magnard, T. Walter, B. Royer, M. Pechal, J. Heinsoo, Y. Salathé, A. Akin, S. Storz, S. Besse, J.-C. Gasparinetti, A. Blais, and A. Wallraff, Deterministic quantum state transfer and remote entanglement using microwave photons, *Nature* **558**, 264 (2018).
- [54] P. Campagne-Ibarcq, E. Zayls-Geller, A. Narla, S. Shankar, P. Reinhold, L. Burkhardt, C. Axline, W. Pfaff, L. Frunzio, R. Schoelkopf, *et al.*, Deterministic remote entanglement of superconducting circuits through microwave two-photon transitions, *Physical review letters* **120**, 200501 (2018).
- [55] G. Dridi, M. Mejatty, S. J. Glaser, and D. Sugny, Robust control of a not gate by composite pulses, *Phys. Rev. A* **101**, 012321 (2020).
- [56] M. A. Nielsen and I. L. Chuang, *Quantum Computation and Quantum Information* (Cambridge University Press, Cambridge, England, 2000).
- [57] R. P. Feynman, An operator calculus having applications in quantum electrodynamics, *Phys. Rev.* **84**, 108 (1951).
- [58] V. S. Popov, Feynman disentangling of noncommuting operators and group representation theory, *Phys.-Usp.* **50**, 1217 (2007).
- [59] K. Blum, *Density Matrix Theory and Applications* (Plenum Press, New York, 1996).